A Study of Spatial Resolution for a Preshower Detector with Aluminum Absorber and Silicon Strip Sampler

Y.H. Chang, A.E. Chen, S.R. Hou, W.T. Lin
Physics Department, National Central University,
Chungli, Taiwan 32054, ROC

T. Antičić, C.-Y. Chien, P.H. Fisher[1]
Department of Physics and Astronomy, Johns Hopkins University,
Baltimore, MD 21218, USA

Abstract

We have studied the spatial resolution of a preshower system with aluminum as absorber and silicon strips as the active sampling detector. The test beam was performed at X3 of the CERN SPS using an electron beam with energies between 4 GeV and 50 GeV. The shower profiles of different beam momenta and absorber thicknesses are compared to full GEANT simulations.

[1]Now at MIT,Cambridge, MA, USA

1 Introduction

In colliding beam experiments, a preshower detector is often considered to provide a position measurement for the physics requirements that may not be achievable by the electromagnetic calorimeter alone. The precision in two-photon separation is important for γ and π^0 identification, and the spatial and angular resolutions are crucial for many physics interests. Preshower detectors using silicon wafer as the active sampling medium have been proposed for the SSC [1] and CMS [2] at the LHC.

This study investigates the effect of positioning the preshower sampling plane behind the framework of the central tracking system. The simplified configurations applied provide general information on the shower characteristics. We chose aluminum as the absorber as it is the most popular framework material. Also its low density sets a bound on the spatial resolution one can achieve, thus the partition size for a preshower sampling detector can be determined.

We use silicon strip detectors behind the aluminum absorber to sample the secondary particles of electromagnetic showers initiated by electrons of 4 GeV to 50 GeV. The silicon strip readout pitch is 50 μm, which provides fine screening of shower profile. The high detection efficiency and low pile-up observed gives a detailed description of the preshower profile.

Several reconstruction algorithms for determining the shower center position have been investigated. There is the basic center-of-gravity (COG) method and others which weight the charge deposited in the silicon wafer with different partition widths to optimize the spatial resolution. The shower profile detected has been compared to a full GEANT [3] simulation. The feasibility of GEANT simulation for spatial resolution is examined.

2 Test beam Setup and Data Processing

The test beam was performed at the X3 beam line of the CERN SPS. The spectrometer magnet was calibrated with momentum precision of $\delta p/p$=1.6% and 0.3% at 4 and 50 GeV respectively [4]. Wider collimator openings were applied at low beam momentum to gain high event rate, which implies a momentum spread of $\delta p/p$=4% and 1% at 4 and 50 GeV respectively. The event trigger had a beam spot of approximately 1×1 cm^2. The beam contamination of hadrons and muons was vetoed by two Cherenkov counters to below 1 % and cross checked by downstream calorimeter.

The two configurations of aluminum absorber and silicon strip detectors are illustrated in Fig. 1. In Setup I, the aluminum absorbers of 0.5, 1.0, 1.4, and $1.7X_0$ were positioned with the backplane fixed at 20 mm from the first sampling wafer; the electron beam energy applied were 4, 10, 20, and 50 GeV. In setup II the absorber was $1.4X_0$ at 50 mm to the first downstream wafer, and the electron

	$N4$	$N9$	$N5$	$J1$	$J2$	$N3$	$C1$	$C2$
readout pitch (μm)	50	50	50	45	80	50	60	60
active width (mm)	6.4	12.8	6.4	17.3	20.5	12.8	23.0	23.0
strip length (mm)	20	80	80	60	60	20	85	85
strip thickness (μm)	320	320	320	300	300	320	300	300
Setup I orientation	y	y	x	y	x	y	y	y
z position (mm)	34	118	132	500	515	660	780	858
Setup II orientation	y	y	–	y	x	y	y	y
z position (mm)	34	493	–	199	217	644	753	843
σ_N (ADC)	1.4	1.3	1.3	1.1	1.1	1.2	2.0	2.2
S/N	17	23	23	27	27	24	18	18
efficiency ϵ	–	.992	–	.991	–	.993	.995	.997
intr. reso. σ_{int} (μm)	6	4	–	9	–	5	7	11

Table 1: Parameters of silicon detectors.

energy was 50 GeV. The wafers before the absorber provide the reference impact position, and the large spacing distances of down stream wafers resolve the pile up problem of shower particles. Relevant geometrical parameters are listed in Table 1. The charge on the readout strips was collected by SVX-D chips [5], each equipped for 128 channels and daisy chained to SRS-SDA modules [6] with readout by an IBM/PC based data acquisition system.

Pedestal events were taken between beam spills during data taking. In the analysis, pedestal events were processed first to produce relative pedestal values between strips. The noise level (σ_N) is the RMS of the pedestal; the average noise over channels of one wafer is used in setting thresholds. The raw ADC also contains a common shift which is uniform through the 128 channels of one SVX-D chip. The charge collected by one readout strip is the ADC value after subtraction of pedestal and common shift.

The induced charge on the silicon wafer from a traversing charged particle is collected by one or more adjacent strips as a cluster. We require a cluster to have the charge of the peak strip to be larger than $3 \cdot \sigma_N$ and the total larger than $6 \cdot \sigma_N$. The signal-to-noise ratio (S/N) obtained are listed in Table 1 along with the noise level.

For clusters that contain more than one strip, the cluster charge is divided into the charges of the left and right strips (Q_l, Q_r) separated by center-of-gravity. The η function is defined as $\eta = Q_r/(Q_r + Q_l)$. As the readout pitch is much smaller than the triggered beam spot, we assume that the event distribution between readout strips are uniform. Therefore, the η distribution $f(\eta)$ represents the nonuniform charge sharing between neighboring strips of a cluster [7].

	$J1$	$N9$	$N3$	$C1$	$C2$
Setup I (μm)	58	–	78	94	102
Setup II (μm)	–	30	41	51	62

Table 2: Precision of reference shower centers.

The η corrected cluster coordinate is derived from the charge integral by $X = p \cdot \int_0^\eta f(\eta) / \int_0^1 f(\eta) + X_0$, where p is the size of readout pitch and X_0 is the offset of the readout strip.

Calibration runs were performed with absorber removed between different beam line configurations. Unweighted linear track fitting was performed on calibration data for alignment between wafers that includes relative offset and tilt angle. The residuals of linear track fitting contain mainly the multiple scattering by silicon wafers and detector intrinsic resolution (σ_{int}). We have employed GEANT to calculate the multiple scattering by silicon wafers. The detector intrinsic resolutions are simulated by additional Gaussian smearing, such that the widths of the residuals in GEANT and the calibration data agree [8]. The detection efficiency (ϵ) of each detector is determined by searching a cluster within a window of ± 2 strips from the linear track projection of the other detectors. Both σ_{int} and ϵ are also listed in Table 1.

3 Shower Profile

We have studied the one dimensional shower profile detected by the preshower sampling wafers behind the absorber. A typical event scan is shown in Fig. 2 of a 50 GeV electron and $1.4X_0$ aluminum absorber. The *reference* shower center position is the linear extrapolation of measurements by wafers before the absorber. The precision of the reference coordinates are determined with respect to the coordinate obtained by linear track fitting. The RMS of reference coordinates obtained from calibration data are listed in Table 2.

Shower events are selected by requiring exactly one cluster on each upstream wafer, and the reference positions on all sampling wafers to be at lease 3 mm away from the boundary of active area. These criteria prevent events mostly from shower initiated before the absorber and provide good shower containment. As the upstream wafers span only a small angle around the normal to the absorber plane, where the back scattering of shower secondaries has the least flux density [9], events containing albedo particles are also selected.

The GEANT simulations have been performed for all beam line setups. In the simulation, the induced charge of a track crossing the silicon wafer is assigned by random sampling on the charge distribution obtained from calibration data. The

distributions of shower total charge collected by $N3$ in Setup I were compared to GEANT simulations and plotted in Fig. 3. The MIP peak is distinguishable in the low multiplicity cases. The unweighted shower profiles of strips above $3 \cdot \sigma_N$ relative to the reference position are shown in Fig. 4.

The pile-up of shower particles is expected in the shower core. The shower profiles sampled by $N9$ and $N3$ of Setup II using 50 GeV electrons and 1.4 X_0 aluminum absorber have been studied for the pile-up effect on the spatial resolution. The shower profiles of reconstructed clusters shown in Fig. 5 have dense core and long tails extending to several millimeters. Good agreement is seen on the unweighted cluster profiles of data (dots) to GEANT (solid lines). The particle density profiles of GEANT are plotted as the dotted lines, for $N9$ it is a factor of 2.5 larger then the density of clusters in the shower core, the charge weighted cluster profiles of data (circles) give better correspondence.

The GEANT simulation describes well the shower core, but lower particle density in the tail causes the discrepancy in the total number of clusters. The number of clusters measured by $N9$ and $N3$ are plotted in Fig. 6 with the distributions of GEANT shown by solid lines. The $N9$, which is positioned directly behind the absorber, sees more clusters than those further downstream. This feature is correctly simulated by GEANT.

As the readout pitch of the silicon strip is 50 μm, the pile-up resolution is limited to 100 μm. Shown in Fig. 7 are the distributions of a) the distance of closest cluster to the reference shower center and b) the average cluster charge versus the distance to the reference shower center. The $N9$ wafer, which is 50 mm away from the absorber, has visible pile-up effect in these distributions.

The long tails of the shower profile can be characterized by the fraction of shower containment versus the covering range centered at the shower core. Shown in Fig. 8 are the distributions of a) the number of clusters integrated, and b) the fraction of charge integrated versus the integration range of $\pm w$ to the reference shower center. In comparison, the results of GEANT are shown by lines. The quick rise of the distributions to the integration range corresponds to the shower core; a proper employment of this feature is important to the shower center reconstruction that is discussed in the next section.

4 Shower Center Reconstruction

The basic algorithm to determine the shower center is the center-of-gravity (COG) method. Considering the pile-up of shower particles, the charge weighted COG would provide a better result. There are, however, problems due to the long tails of shower profile that introduce large fluctuations in the COG by particles far off the center.

The following two algorithms described for shower center reconstruction are applied to data of Setup I that has a energy scan from 4 to 50 GeV with a 1.4

X_0 absorber, and a scan of absorber thickness from 0.5 to 1.7 X_0 with 50 GeV electrons. The *window* algorithm locates the shower center on the sampling wafer by the following procedure:

i. searching through all strips above $3 \cdot \sigma_N$, the first median (m_1) is the position of the middle strip and the corresponding RMS is $\sigma_{m_1} = (\sum_i (x_i - m_1)^2 / n)^{1/2}$ where x_i is the position of i'th strip of the total of n;
ii. locating the second median (m_2) which is the position of the middle strip within the region of $m_1 \pm \sigma_{m_1}$;
iii. the shower center is the unweighted COG in the window of $m_2 \pm n_w$ strips.

The *density* algorithm illustrated below is intended to keep the spatial resolution of the 50 μm readout pitch, while extending the range of charge collection by combining the charge of several strips. For the i'th strip, the charge density d_i is assigned as the sum of charge of adjacent $\pm n_d$ strips. The shower center is reconstructed by:

i. locating the strip of maximum d_i above a threshold of $3 \cdot n_d \cdot \sigma_N$, clustering the neighering d_i above $1 \cdot n_d \cdot \sigma_N$, and requiring the total sum to be larger than $6 \cdot n_d \cdot \sigma_N$;
ii. the shower center is the d_i weighted COG of the shower cluster.

The shower centers reconstructed by these two algorithms were fitted to Gaussian distributions on the shower core. Illustrated in Fig. 9 and Fig. 10 are the RMS values obtained by sampling wafers behind absorber for all beam line configurations of Setup I. The parameters applied are n_d=4 and n_w=4 for density and window algorithms respectively, corresponding to a full width of 400 μm. The systematic uncertainty is dominated by the precision of determining the reference coordinate by extrapolation followed by the multiple scattering by silicon wafers. The solid line plotted in Fig. 9 demonstrates the RMS of extrapolation coordinate relative to the reconstructed cluster position of calibration runs. The results obtained from GEANT simulation are illustrated by the dotted lines. In the simulation, the detector intrinsic resolution of each detector and reference coordinates by extrapolation are smeared to agree with calibration data. The shower center of GEANT is in general more precise than data, with reduced RMS of up to 10%. The two algorithms tested give compatible results. The RMS obtained increases slowly with n_w and n_d within a corresponding window of up to several millimeters.

A more elaborate method that takes into account the window width weighting on the fraction of total charge would improve the spatial resolution of the reconstructed shower center. The *charge-weighted window* algorithm is applied on the data of Setup II of 50 GeV electron and 1.4 X_0 absorber. The shower center is reconstructed by:

i. first moving a window of size W_{cut} along the strips to search for the location of the maximum fraction of charge content in the window;

		Q_{cut}=0.25,W_{cut}=200μm			Q_{cut}=0.25,W_{cut}=600μm		
		σ_c (μm)	σ_t (μm)	R_c(%)	σ_c (μm)	σ_t (μm)	R_c(%)
$N9$	data	97$\pm$4	610$\pm$34	54$\pm$5	150$\pm$4	828$\pm$62	72$\pm$4
	mc	72$\pm$2	466$\pm$34	64$\pm$3	130$\pm$2	796$\pm$76	79$\pm$3
$N3$	data	186$\pm$10	957$\pm$50	43$\pm$7	206$\pm$7	990$\pm$50	51$\pm$5
	mc	159$\pm$4	927$\pm$30	49$\pm$4	180$\pm$4	870$\pm$30	57$\pm$3

Table 3: Results of the fit to two Gaussians on the distribution of reconstructed shower center of $N9$ by the *charge-weighted window* algorithm.

ii. requiring the charge fraction to be larger than Q_{cut}; otherwise the window size is increased and the search started again until a window size is big enough to contain charge above Q_{cut};
iii. the shower center is the charge weighted COG in the window.

Shown in Fig. 11 are the distributions of reconstructed shower center to the reference coordinates of $N9$ and $N3$ with W_{cut}=200 μm and Q_{cut}=0.25, dotted lines are those of GEANT. The solid lines are the fit to a sum of two Gaussian functions with RMS corresponding to the core(σ_c) and tail(σ_t) parts. The RMS of the fit and the fraction (R_c) of the events in the core Gaussian for Q_{cut}=0.25 and W_{cut}=200 and 600 μm are listed in Table 3. In comparison, the corresponding values of GEANT are also listed.

The $N9$ wafer in Setup II has a strong pile-up in the shower core. The stability of the charge-weighted window algorithm for the shower center has been tested using various threshold values of W_{cut} and Q_{cut} on $N9$ which has a large deviation in the charge fraction to the window size due to the pile-up. The results listed in Table 4 include two sets with one threshold fixed in each. We found that the resolution and R_c are not sensitive to Q_{cut}; it is, however, sensitive to W_{cut}.

5 Summary

We have investigated the spatial resolution for a preshower system using silicon strips as the active medium to detect electron showers initiated in aluminum absorber. The high detection efficiency and fine sampling of the shower profile provided the precision at the physics limit for the shower center reconstruction. It is shown in the charge-weighted window algorithm that the fraction of events in core Gaussian increases with the window size. However, a smaller sampling width is necessary to achieve a high spatial resolution.

The shower profiles are compared to GEANT simulations with good agreement seen in the shower core. There is approximately a 10% lower particle density

W_{cut}=200μm							
Q_{cut}(%)	15	20	25	30	35	40	45
σ_c (μm)	89	92	97	111	118	122	125
R_c	54%	55%	56%	57%	56%	52%	47%
Q_{cut}=0.25							
W_{cut} (μm)	200	300	400	500	600	700	800
σ_c (μm)	97	104	114	132	150	166	181
R_c	56%	59%	63%	68%	71%	73%	75%

Table 4: Fit results on the distributions of shower center by the *charge-weighted window* algorithm of different W_{cut} and Q_{cuts} thresholds.

simulated in the shower tails. The reconstructed shower center is up to 10% more precise than the one obtained on data.

Acknowledgements

We are grateful to the CERN SPS staff for their technical assistance. We thank our colleagues at ERSO for the manufacture of many of the silicon wafers. This work was partially supported by the Taiwan National Science Council (NSC82-0212-M-008-114), Tsu Yuan-Chi memorial foundation and National Science Foundation (PHY-9221761).

References

[1] A. Arodzero et al., IEEE Trans. Nucl. Sci. 40 (1993) 563.

[2] P. Aspell et al. (RD36 Collaboration), CERN-PPE/95-151 (Sep. 1995); A. Cheremukhin et al. (RD36 Collaboration), CERN-ECP/94-9 (Sep. 1994).

[3] GEANT Version 3.21; R. Brun et al., CERN DD/EE/84-1 (September 1987); CERN Program Library Long Writeup W5013 (March 1994).

[4] B.Borgia, K.Freudenreich, D.Luckey and G.Sauvage; New measurement of the *Bdl* of B2 magnets in X3 beam line; Memorandum (October 1989).

[5] S.A. Kleinfelder et al., IEEE Trans. Nucl. Sci. 35 (1988) 171; N. Bacchetta et al., Nucl. Instr. Meth. A 324 (1993) 284.

[6] F.A. Kirsten, C. Haber, Proc. IEEE Trans. Nucl. Sci. 37 (1990) 288.

[7] E. Belau et al., Nucl. Instr. and Meth. 214 (1983) 253.

[8] Y.H. Chang et al., Nucl. Instr. Meth. A 363(1995) 538.

[9] L.A. Khein, A.V. Plyasheshnikov, Nucl. Instr. Meth. A 342 (1994) 451.

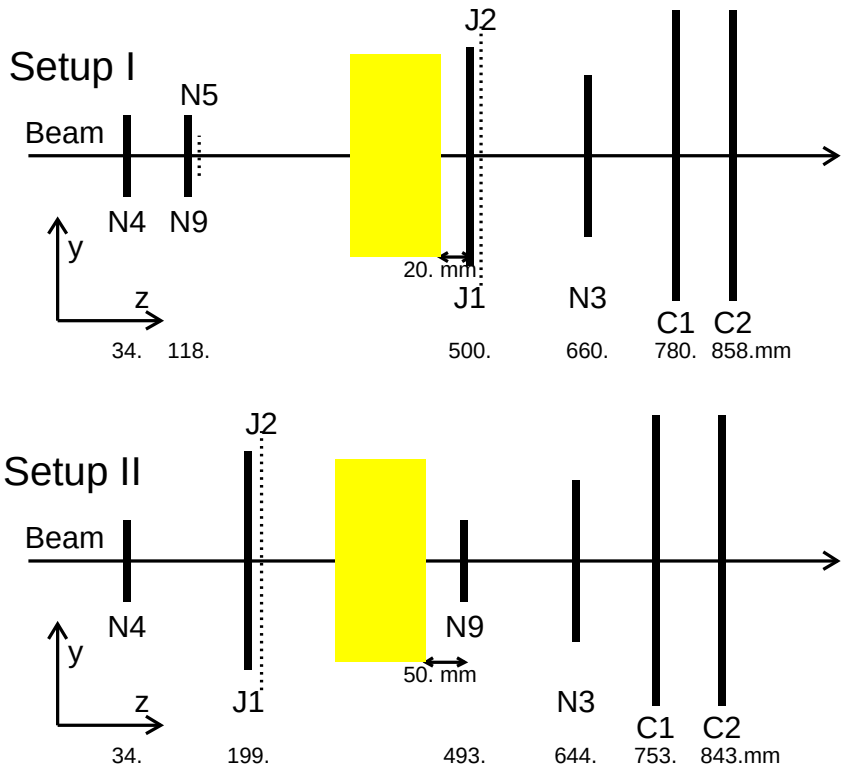

Figure 1: Test beam setups.

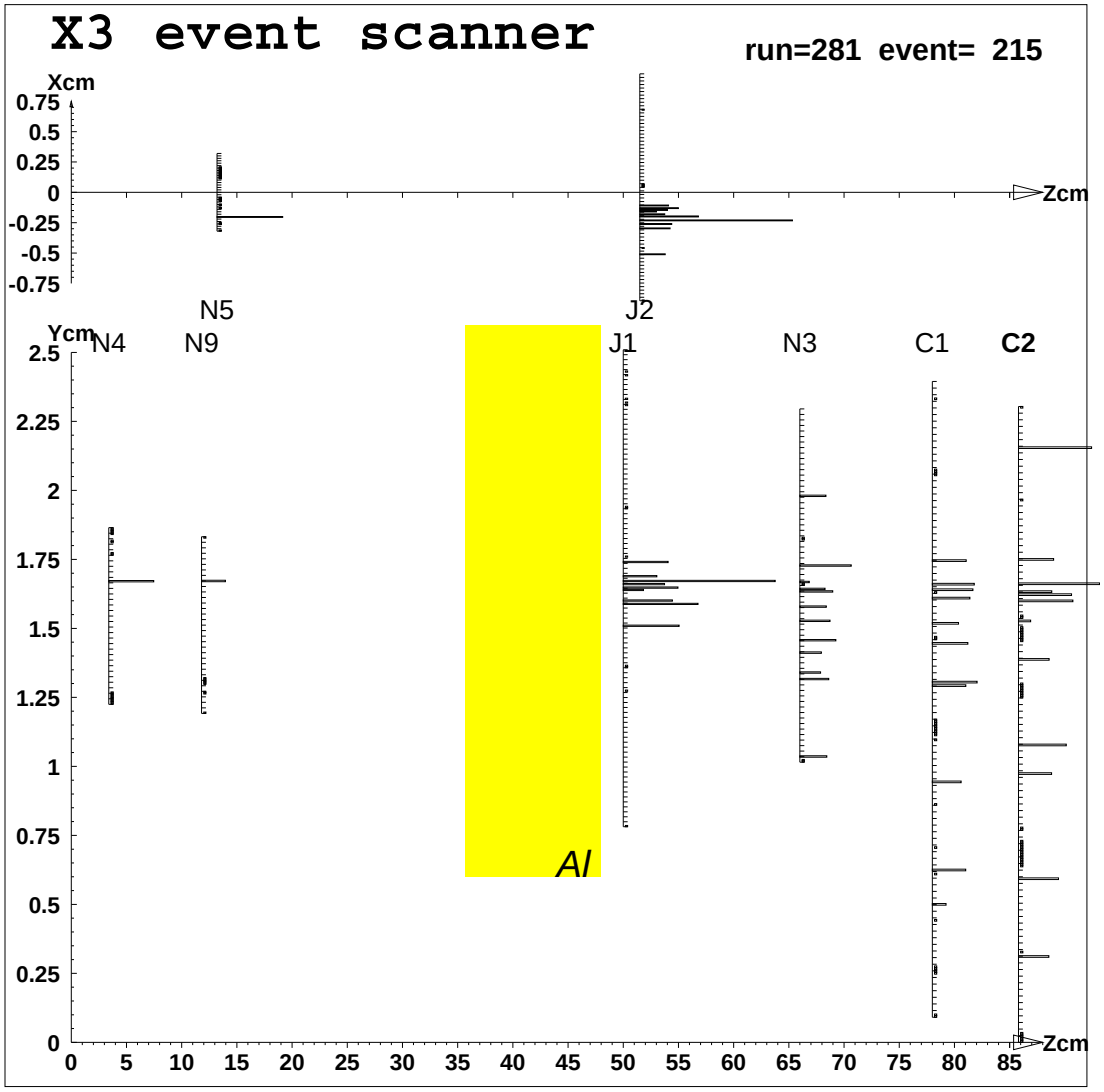

Figure 2: Event display of a typical shower event of a 50 GeV electron and $1.4X_0$ aluminum absorber. Each spike is a reconstructed cluster with the height proportional to the cluster charge.

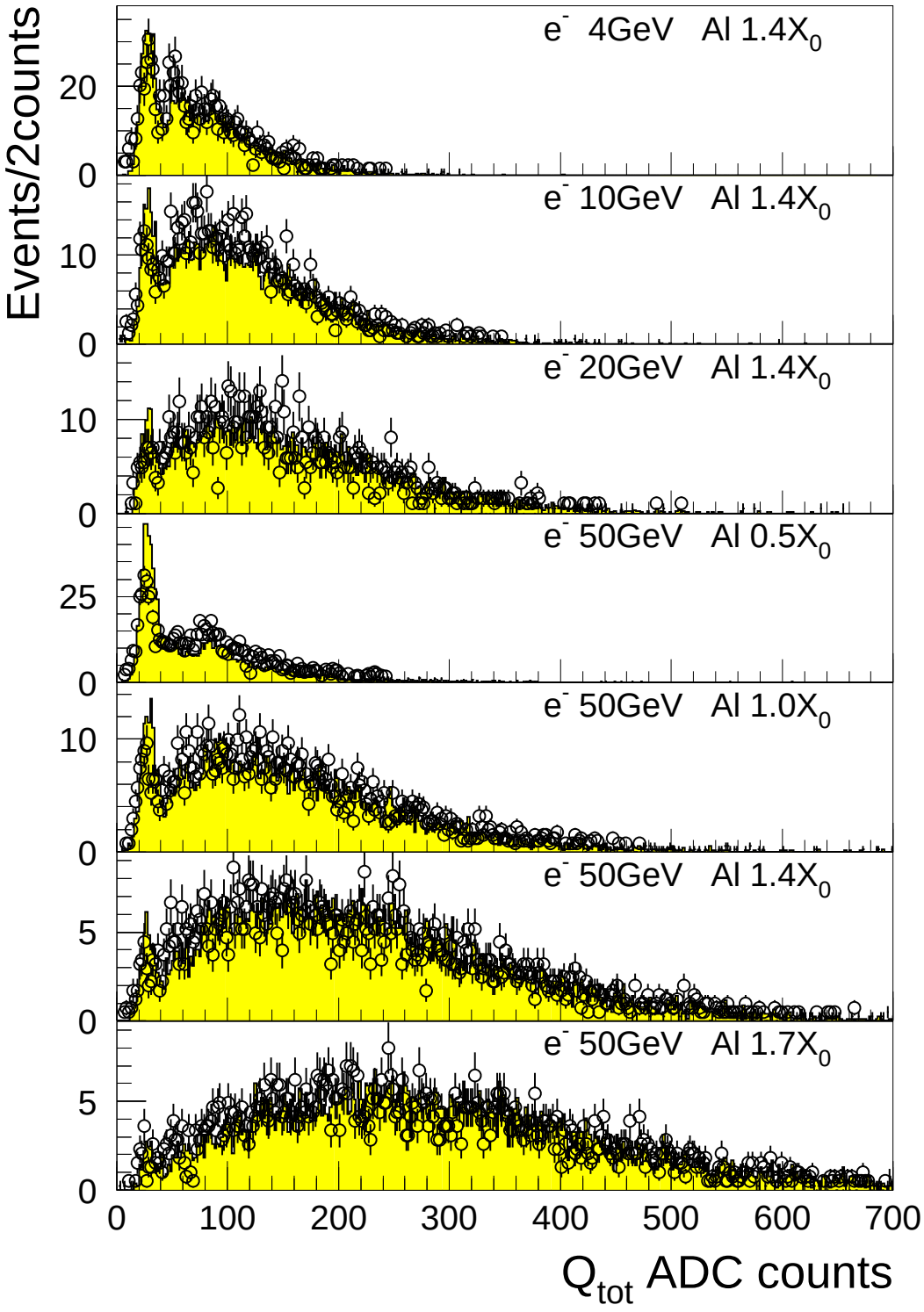

Figure 3: Shower total charge collected by $N3$ (circles) in comparison with GEANT simulation (shaded histogram).

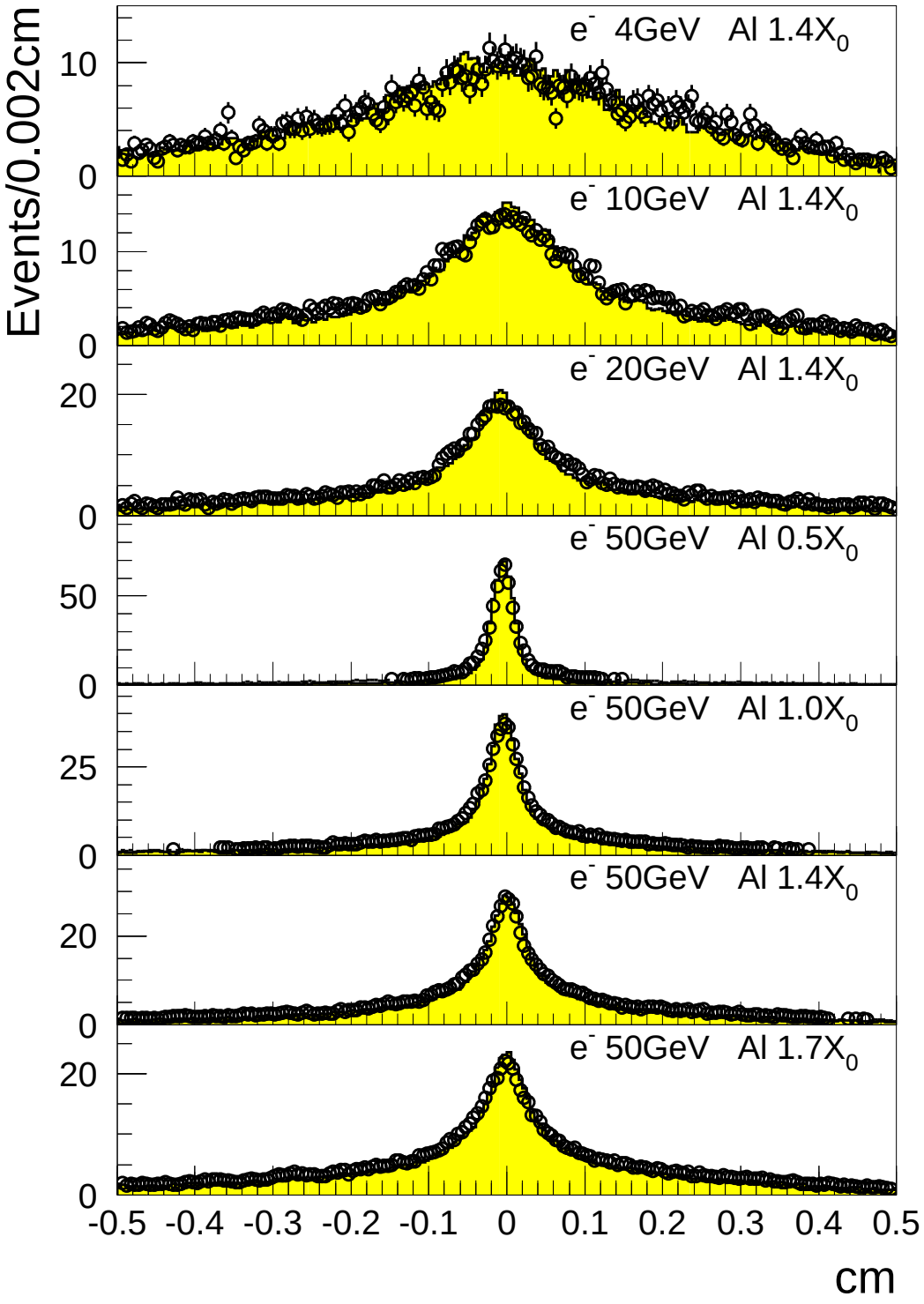

Figure 4: Shower profile of strips above $3 \cdot \sigma_N$ measured by $N3$ (circles) in comparison with GEANT simulation (shaded histogram).

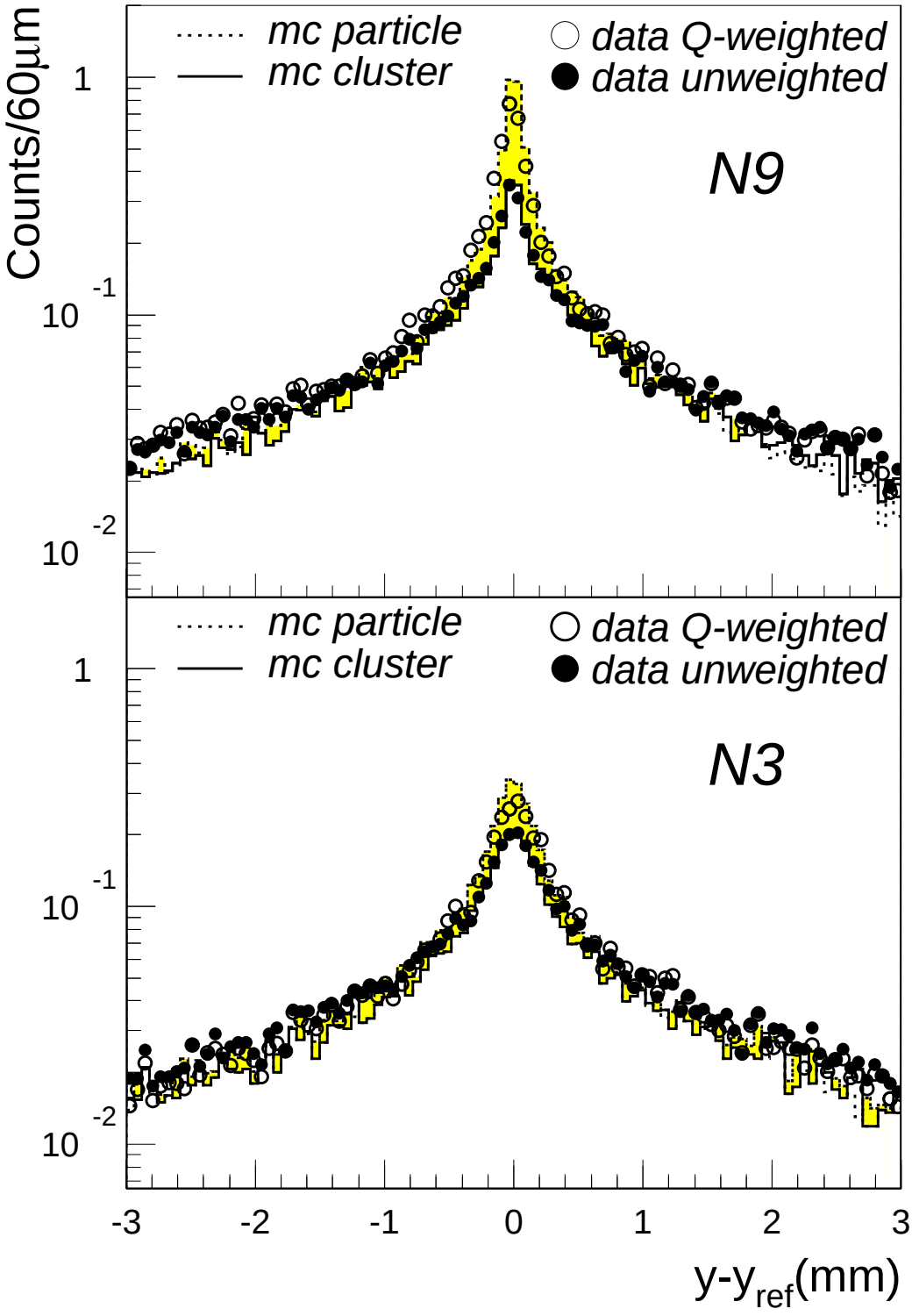

Figure 5: The $N9$ and $N3$ measurements of unweighted cluster profile (dots) and charge weighted cluster profile (circles) in comparison with GEANT simulation of unweighted cluster profile (solid line) and particle density profile (dotted line).

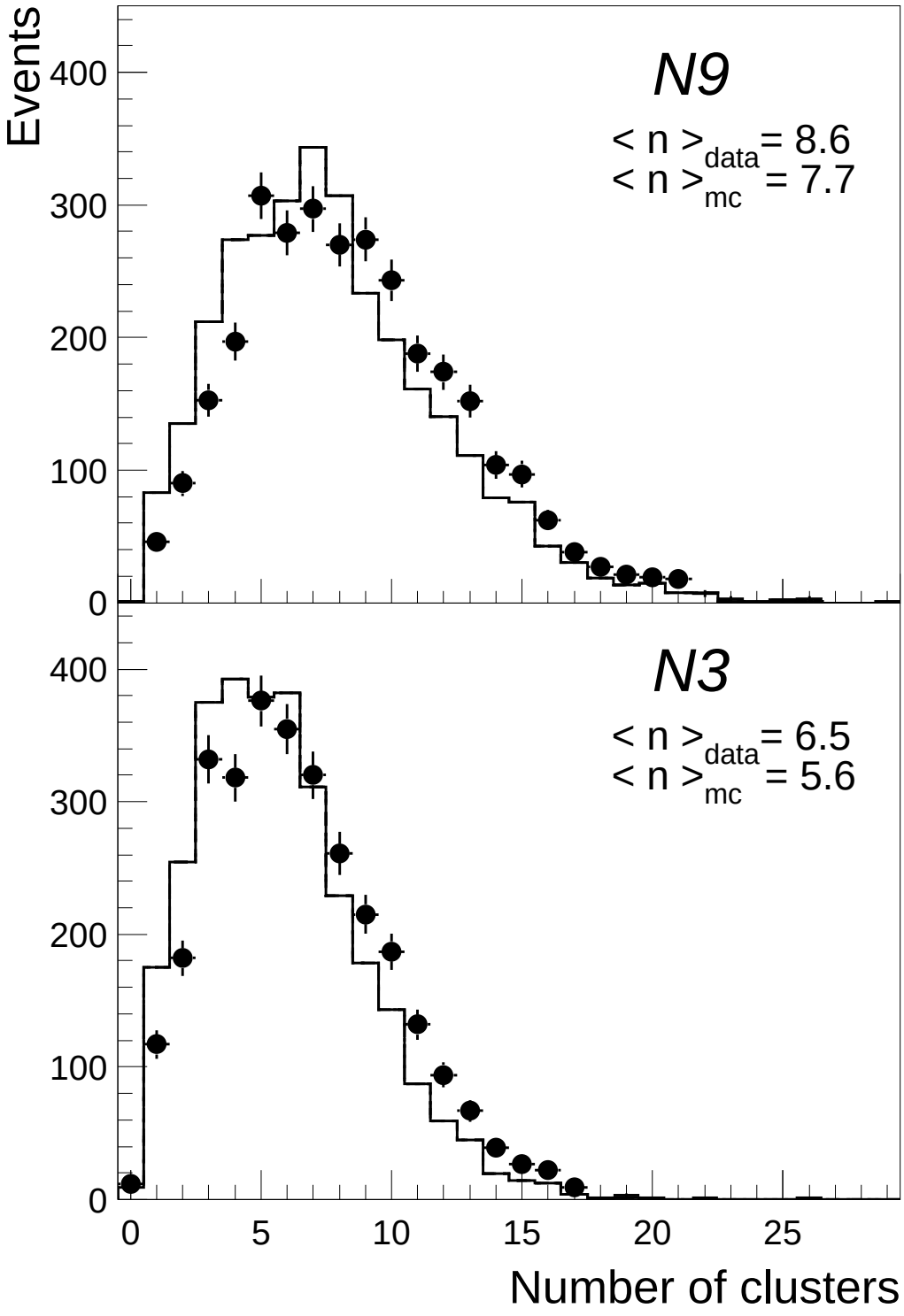

Figure 6: Number of clusters measured by $N9$ and $N3$ (dots) in comparison with GEANT simulation (histogram).

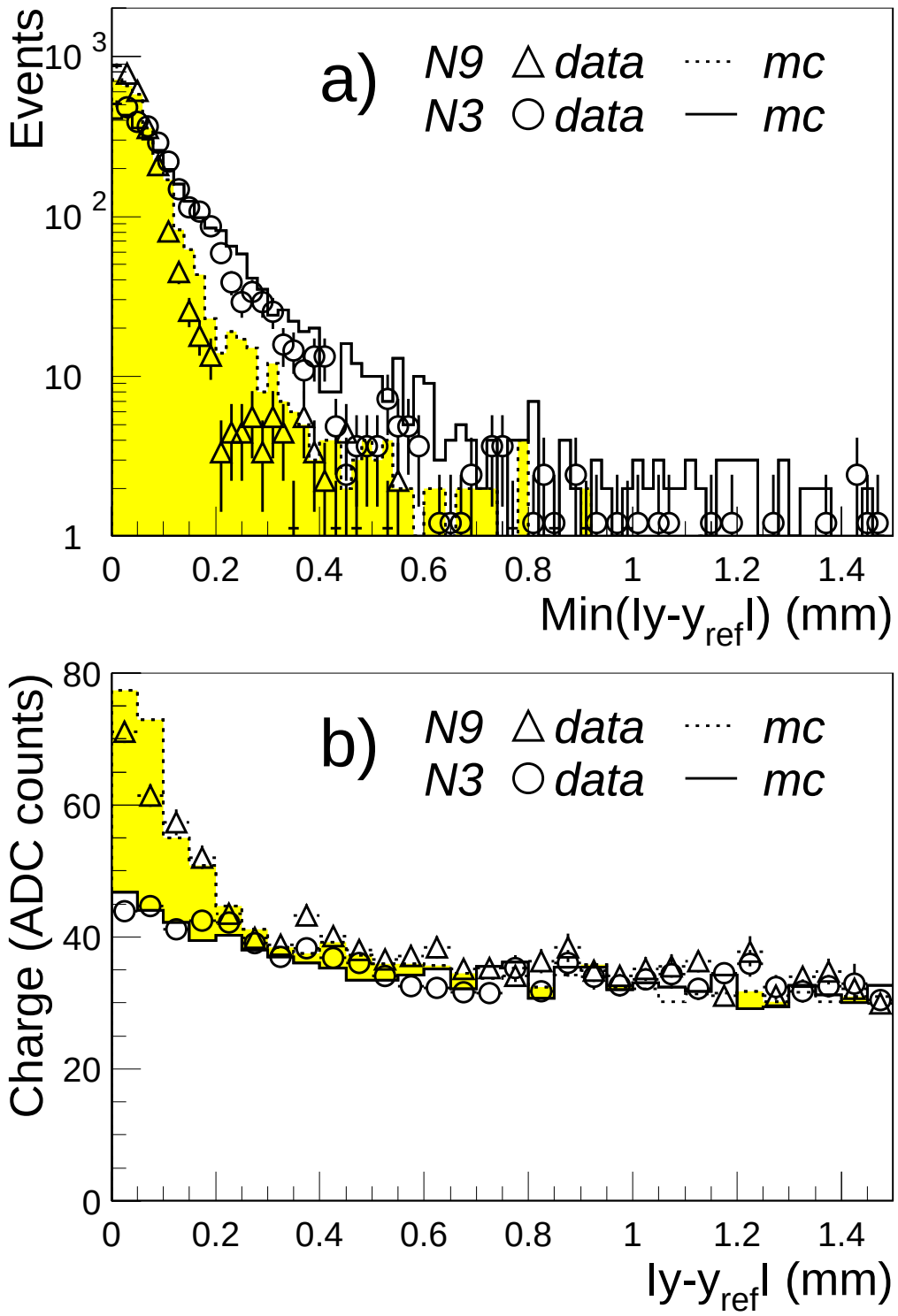

Figure 7: The pile-up effects seen by $N9$ and $N3$ on a) the distance of closest cluster to the reference shower center and b) the average cluster charge versus the distance to the reference shower center.

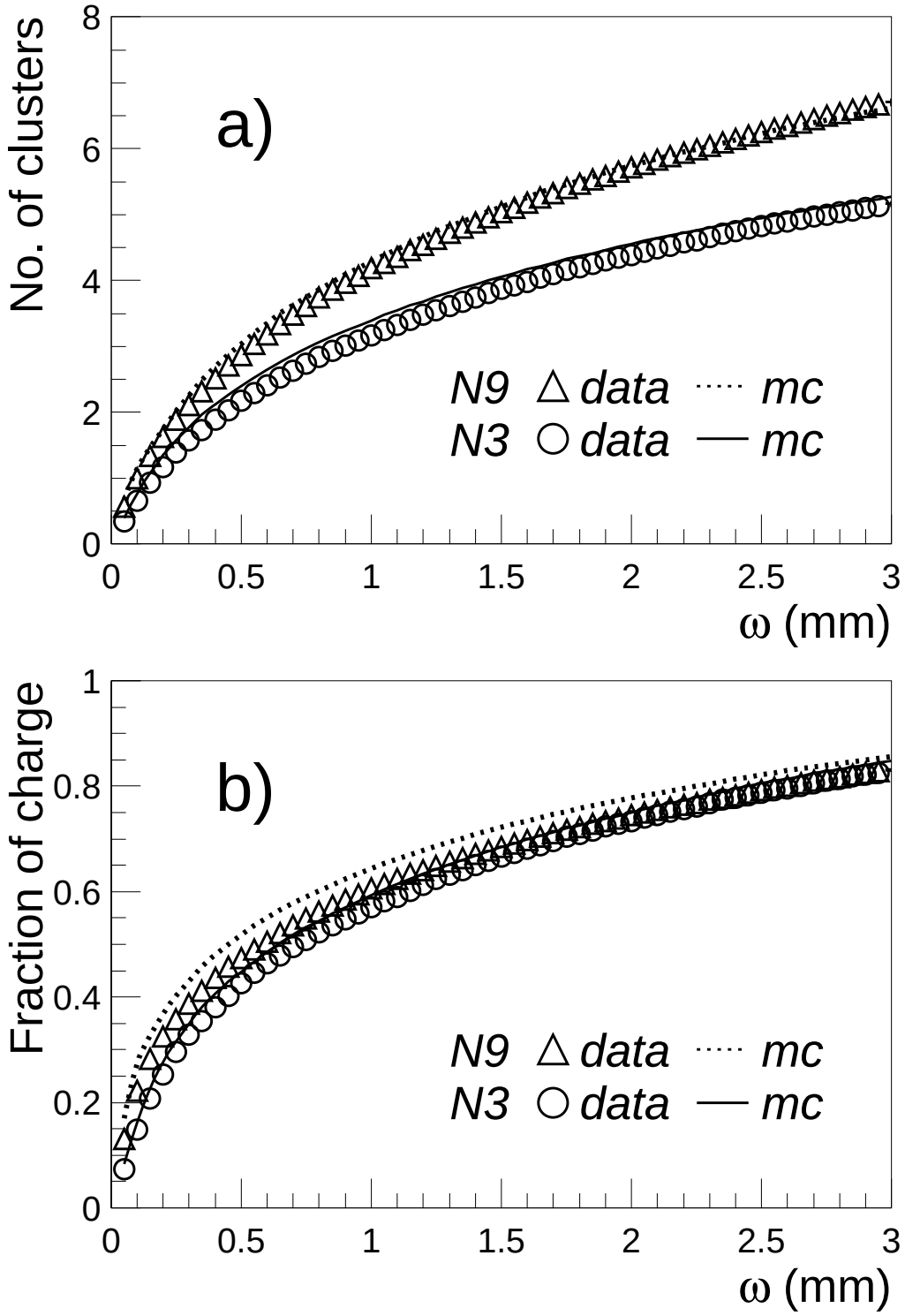

Figure 8: Integrated a) number of clusters and b) fraction of charge versus the integration range $\pm w$ to the reference shower center.

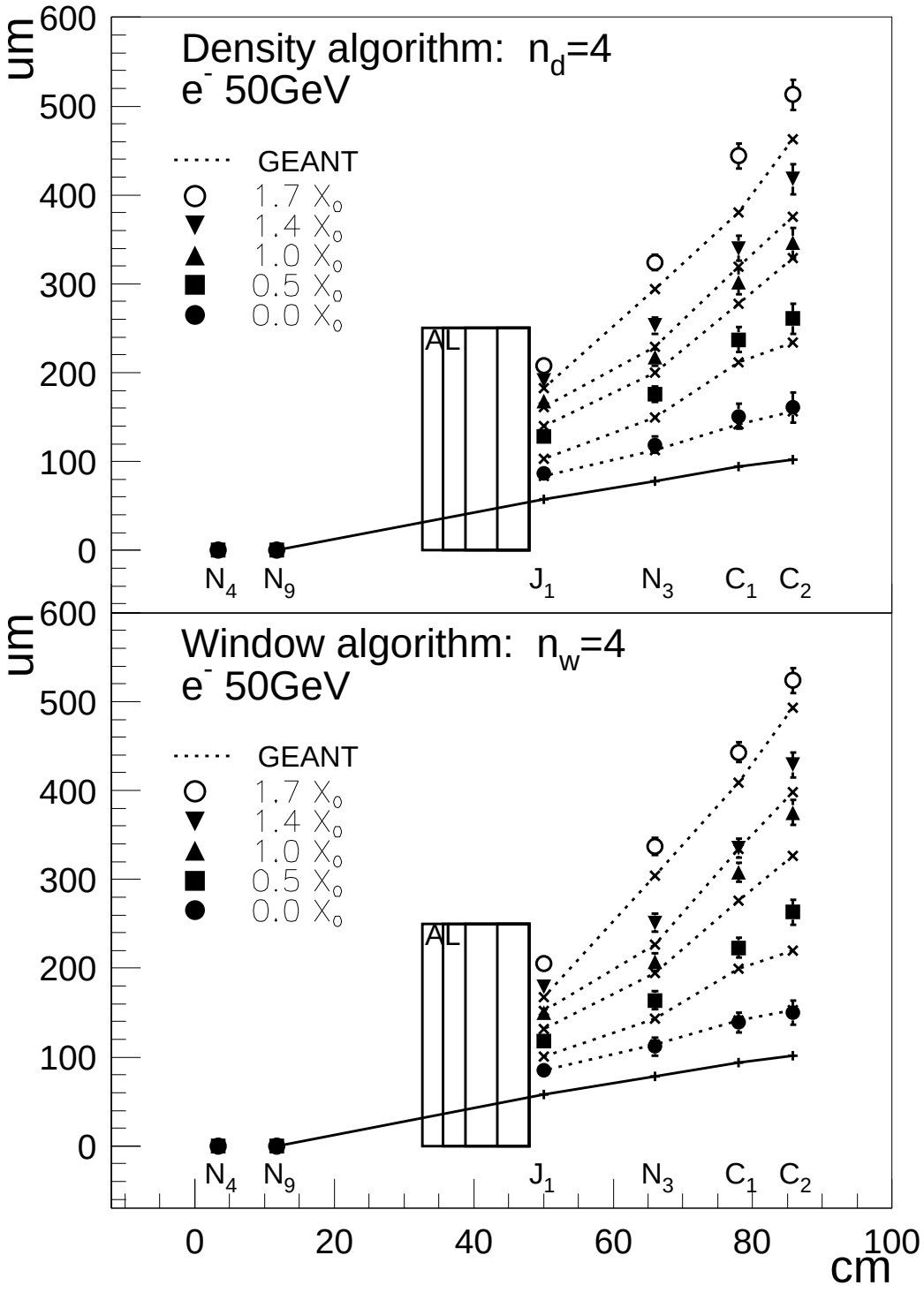

Figure 9: RMS of Gaussian fit on the distributions of shower center by *window* and *density* algorithms for 50 GeV electrons with different absorber thicknesses. The solid lines indicate the precision of reference shower centers.

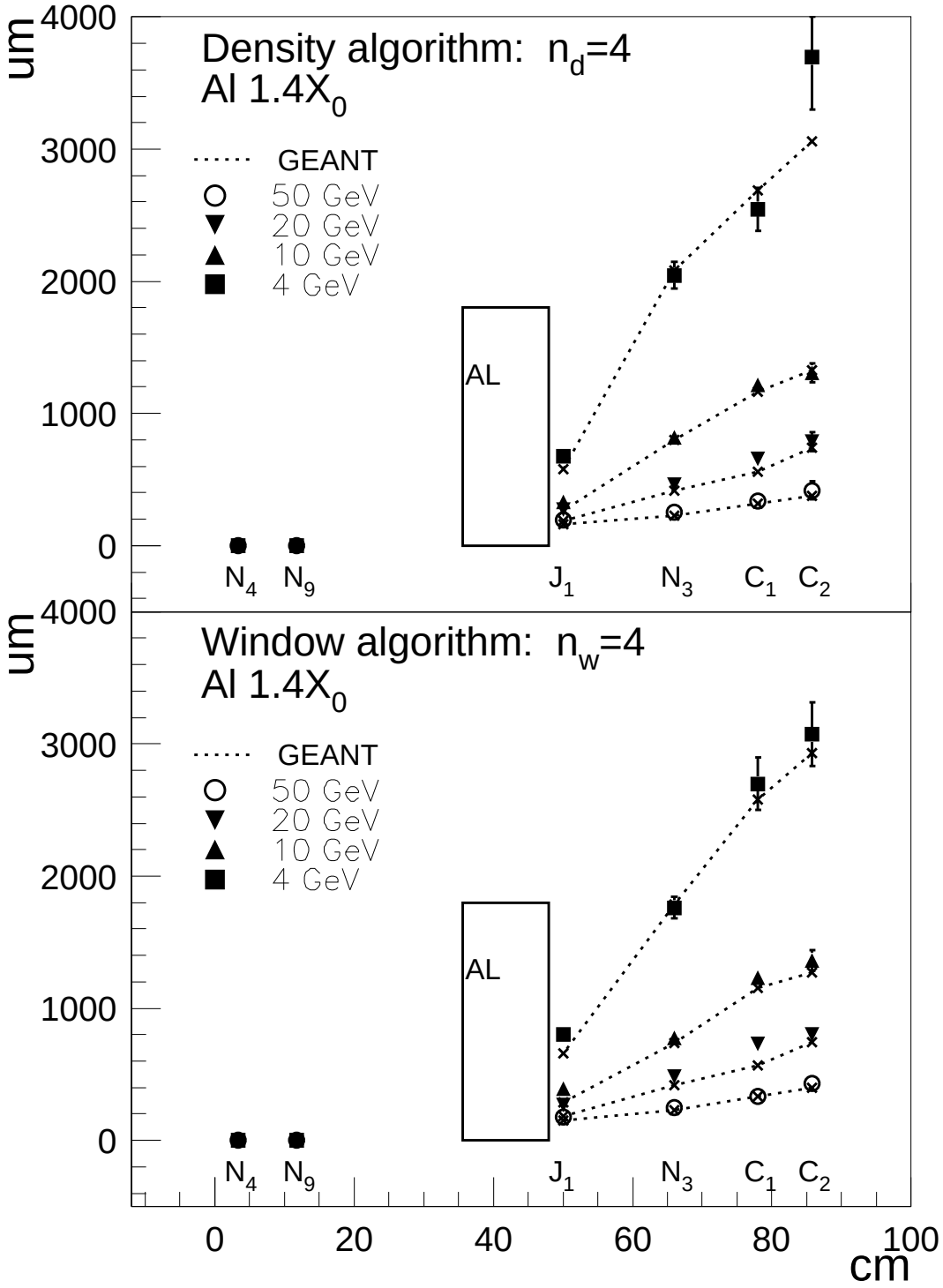

Figure 10: RMS of Gaussian fit on the distributions of shower center by *window* and *density* algorithms for 1.4 X_0 absorber with different beam energies.

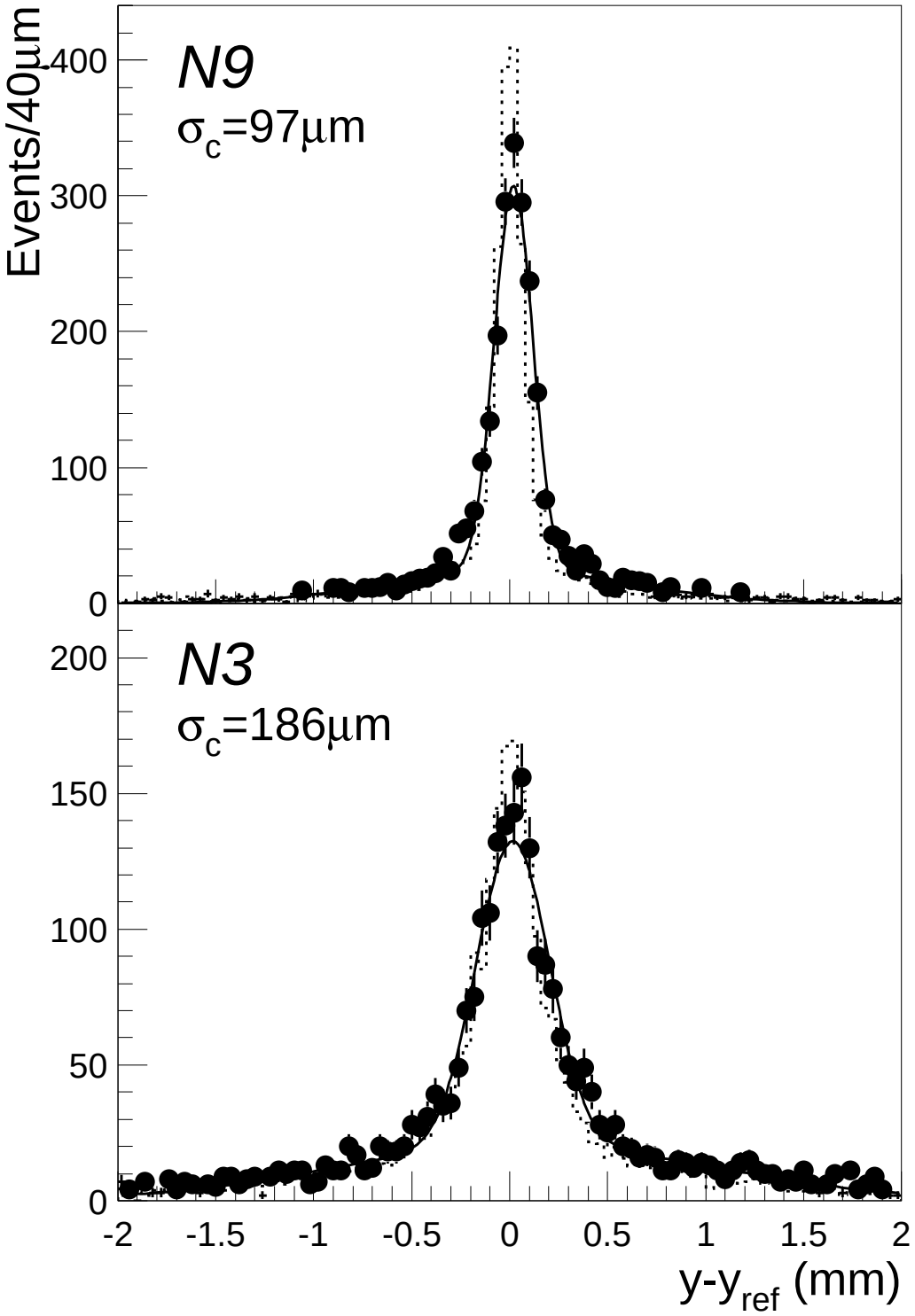

Figure 11: Distributions of the reconstructed shower center of $N9$ and $N3$ by the *charge-weighted window* algorithm in comparison with GEANT simulation (dotted lines). Solid lines are the fit to two Gaussian distributions.